An Integrated Hybrid Power Supply For Distributed Generation Applications Fed by Non Conventional Energy Sources

K. Krishna Reddy [1*], S. Hareesh [2]

[1,2] Department of EEE, Mother Theresa Institute Of Engineering and Technology (A),Palamaner, JNTUA, AP, India ; krishnareddy206@mtieat.org

Abstract: This paper proposes a new technique for energy managing in hybrid power systems. The proposed management system is designed to manage the power flow between the hybrid power system in order to satisfy the load requirements based on artificial neural network (ANN) and fuzzy logic controllers. The neural network controller is employed to achieve the maximum power point tracking (MPPT) for different types of sources like Photovoltaic(PV), wind energy and Fuel cell at DC-link.. The developed fuzzy logic controller (FLC)-based MPPT method and ANN based method   was assessed using a hybrid system comprised PV panels, wind turbine (WT) and Fuel Cell with DC–DC converters. The dynamic behaviour of the proposed model is examined under different operating conditions. The analysis of the proposed hybrid system provides higher power as compared to PV, WT and FC systems at different loads. This research is utilized for the stand-alone system as well as a grid. ANN gives a better performs compared to the Fuzzy in the MPPT method for the PV panels, wind turbine (WT) and Fuel Cell with DC–DC converters for the DC loads. The result analysis of the Fuzzy and the ANN are simulated in the MATLAB/Simulink.

Keywords: Hybrid Power Supply, ANN, ML, Python, Non-Conventional Energy Sources.

1. Introduction

On January 30, 2020, the International Health Regulations Emergency Committee of the World Health Organisation(WHO) declared the outbreak of the performing complaint from this new CoV called COVID- 19, as a" public health exigency of transnational concern".

Renewable energy sources have been found to be promising energy sources toward building a sustainable and environment friendly energy economy in the next decade. Among these renewable energy sources, solar and wind energy which are two of the most promising renewable power generation technologies. The growth of PV and wind power generation systems has exceeded the most optimistic estimation. In addition, the dynamic interaction between the load demand and the renewable energy source can lead to critical problems of stability and power quality that are not very common in conventional power systems. Therefore, managing the flow of energy throughout the hybrid system is essential to increase the operating life of the membrane and to ensure the continuous energy flow. Overcome this problem to motivate society toward the research and development of alternative energy sources. Several types of non-

conventional energy sources such as solar photo-voltaic (PV) and wind turbine (WT) are established in the last decade. They are not only clean and abundant in nature but also well developed, cost-effective and widely used [1]. Apart from these sources, fuel cells (FC) are also used to handle increasing power demand. In the literature, there are a few studies related to energy management of hybrid power system [2]. Among them, Wang and Nehrir [3], proposed a power management strategy for an DC-linked hybrid wind/PV/FC energy system. in this paper author presented a power management strategy which studied power fluctuations in a hybrid PV/wind turbine/FC power system Ahmed et al. [4]. in the paper, proposed a power management strategy algorithm which dealt with a hybrid PV/wind/FC power system containing an ultra-capacitor bank in Onar et al. [5],.

However, all of the early mentioned methods have used conventional approaches for controlling hybrid power systems, such as linear PI controller which has afterwards been proven its instability in handling various changes in weather conditions [6,7]. The hybrid renewable energy system (HRES) provides an outstanding opportunity for

distributed power generation. Among them, Wang and Nehrir [8] proposed a power management strategy for an AC-linked hybrid wind/PV/FC energy system, Ahmed et al. [9] presented a power management strategy which studied power fluctuations in a hybrid PV/wind turbine/FC power system, and Onar et al. [10] proposed a power management strategy algorithm which dealt with a hybrid PV/wind/FC power system containing an ultra-capacitor bank. Wind turbine energy systems are the fastest developing system innovation as far as rate of yearly development of introduced limit per innovation source. The wind turbine energy system is the best option to present-day innovation particular and efficient to introduce [12, 13]. PV systems are versatile from little to substantial and simple to incorporate with existing DC–DC power converters [14–18]. The proposed method introduces an online energy management by a hierarchical controller between four energy sources comprises PV panels, wind turbine, Fuel cell. The block diagram of the developed hybrid power system is shown in Fig1. WT and PV have gotten to the most encouraging exchange wellsprings of energy because of the way that their sources are supportable and free. Power generation through renewable energy sources with DC–DC converters provides stable results using MPPT control method.
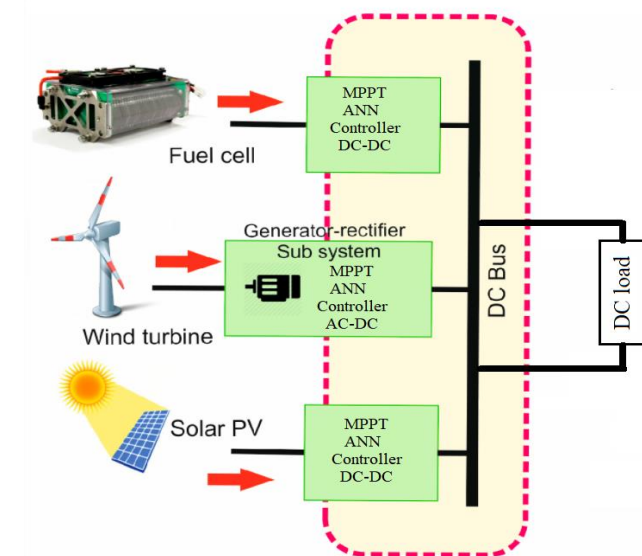

Figure.1: Energy Conversation Module

There are a few methods to seek the best estimation of a capacity [22, 23], where the Perturb and Observe (P&O) MPPT technique is frequently utilized one in light of its straightforward determination, and different MPPT techniques have been proposed for FC system [24–26]. Moreover, previous studies showed [8,9] that using the artificial intelligence in the hybrid vehicle can control the FC system within a specified high-efficiency region. Hence, this paper presents an adaptive management strategy for power flow in stand-alone hybrid power

systems based on fuzzy logic and neural network. In this paper, apply the MPPT control method for achieving the maximum power of PV, WT and FC system and comprise all systems at DC-link which provide the combined power that is hybrid power.

2. Related Work

Mathematical Analysis Of Photo-Voltaic Pv , Wind Turbine And Fuel Cell Systems.

The equivalent circuit of a PV cell is shown in Fig.2. Practically, PV cells are grouped in larger units called PV modules and these modules are connected in series or parallel to create PV arrays which are used to generate electricity in PV generation systems. The current source Iph represents the cell photocurrent. Rsh and Rs are the intrinsic shunt and series resistances of the cell, respectively. The equivalent circuit for PV array is shown in Fig. 2.
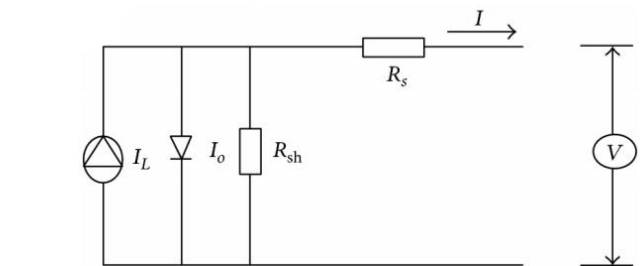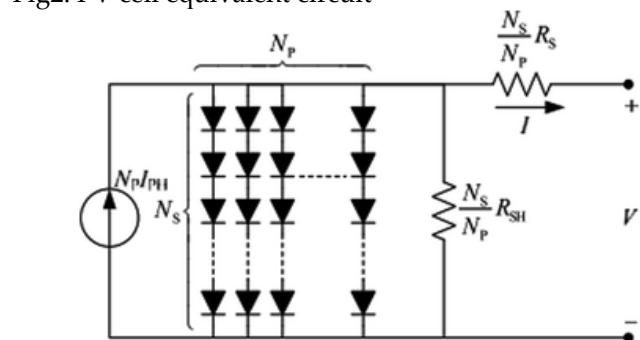

Fig2. PV cell equivalent circuit

Fig 3. Equivalent circuit of solar array.

The voltage–current characteristic equation of a solar cell is provided as
$$Iph=[Isc+Ki(T−298)]×Ir/1000 Iph=[Isc+Ki(T−298)]×Ir/1000$$
(1)
Here, Iph: photo-current (A); Isc: short circuit current (A) ; Ki: short-circuit current of cell at 25 °C and 1000 W/m2; T: operating temperature (K); Ir: solar irradiation (W/m2).

Module reverse saturation current Irs:
$$Irs=Isc/[exp(qVOC/NSknT)−1]$$

Here, q: electron charge, = $1.6 × 10^{−19}$C; Voc: open circuit voltage (V); Ns: number of cells connected in series; n: the

ideality factor of the diode; k: Boltzmann's constant, = 1.3805 × 10–23 J/K.

The module saturation current I0 varies with the cell temperature, which is given by:

$$I_0 = I_{rs}\left[\frac{T}{T_r}\right]^3 \exp\left[\frac{q \times E_{g0}}{nk}\left(\frac{1}{T} - \frac{1}{T_r}\right)\right]$$

Here, Tr: nominal temperature = 298.15 K; Eg0: band gap energy of the semiconductor, = 1.1 eV; The current output of PV module is:

$$I = N_P \times I_{ph} - N_P \times I_0$$
$$\times \left[\exp\left(\frac{V/N_S + I \times R_s/N_P}{n \times V_t}\right) - 1\right] - I_{sh}$$

With

$$V_t = \frac{k \times T}{q}$$

$$I_{sh} = \frac{V \times N_P/N_S + I \times R_S}{R_{sh}}$$

Here: Np: number of PV modules connected in parallel; Rs: series resistance (Ω); Rsh: shunt resistance (Ω); Vt: diode thermal voltage (V).

Wind turbine modelling

Wind turbine induction generator (WTIG) system has two convert processes. First, convert wind energy into mechanical energy, and this mechanical energy is converted into electrical power. The cross section in Fig. 3 shows the arrangement of internal parts of a wind turbine system. WT gets the air from its rotor sharp edges and after that trades the power from rotor edges to rotor axis point. In order to achieve the high rpm of the shaft connected to the generator, gear box is used. Mechanical energy available at the shaft which is connected to the electrical generator gets transformed into electrical energy.
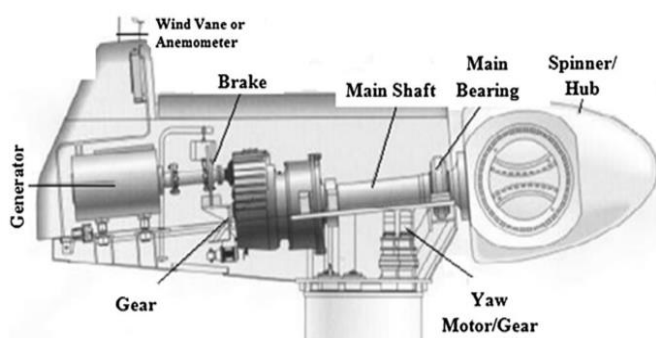

Fig. 3 Cross section showing the arrangement of internal parts of a wind turbine

In case, the wind condition varies and then the power obtained from variable conditions is arranged in the form of matrices. Finally, the electrical energy which has been obtained from the system can be expressed by an outstanding cubic equation as shown in Eq. (4) [28].

$$P_m = \frac{1}{2}C_p(\lambda, \beta)\rho A V^3$$

where Pm = mechanical power (W), Cp = power coefficient, q = air density (kg/m3), A = area swept through rotor blades (m2), k = tip-speed ratio, V = wind speed (m/s), b = pitch angle (rad). It is examined through aerodynamic laws, and therefore, power in air flow can convert from one turbine type to another.

Power in air flow is given as:

$$P_{air} = \frac{1}{2}\rho A V^3$$

Aerodynamic efficiency of the wind turbine is nominated through coefficient function of power, Cpðb; kÞ, given by:

$$C_p = \frac{P_m}{P_w}$$

where Pw = input power of WT and Cp = actual power extracted through the wind turbine, Pitch angle (b) and tip speed ratio (k). b is an angle by which the blade is twisted besides its longitudinal axis. k is well defined as the ratio in favour of the rotor speed toward wind speed is represented by:

$$\text{TSR }(\lambda) = \frac{R}{V}\omega_s$$

Power extracted through wind turbine rotor is known by:

$$P_{wt} = C_p \cdot P_{air}$$

where Pwt = power extracted through wind turbine rotor (W), xs = rotor-shaft speed (rad/s), R = radius of rotor swept area (m). The ideal scenario of an infinite number of blades and no losses, the upper limit for the aerodynamic rotor coefficient is equivalent to Betz limit Cpmax = 0.593.

Mathematical model of a fuel cell

Proton exchange membrane fuel cell (PEMFC) is represented in Fig. 4. FC includes PEM, gas diffusion layer (GDL), catalyst layer (CL), gas channel (GC) and current collector (CC) of anode and cathode.
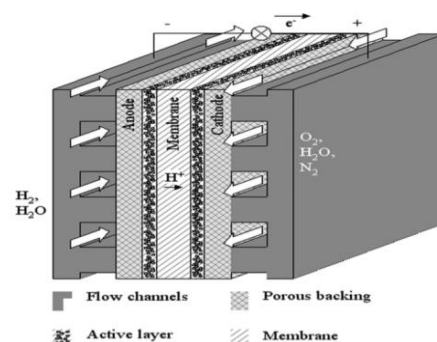

Fig. 4 Model representation of a proton exchange membrane fuel cell.

3.3.1 Model equations of fuel cell Model of basic fuel cell constitute mass, thermal energy, momentum, species and charge. This model is based on principles of five equations. Equations are coupled among electrochemical process throughout source terms in order to define

K. Krishna Reddy, et, al.

reaction kinetics and electro-osmotic drag during polymer electrolyte. The equations can be specified by vector form.

Maximum power point tracking techniques

The productivity of WT, solar PV and FC is improved by MPPT technique when they set to work for the purpose of greatest power. There are distinctive methods of MPPT. The most well-known MPPT techniques are Perturb and Observe (P&O), incremental conductance technique (INC), the fuzzy logic controller (FLC) [30–37] and neural network (NN) control methods. Beginning photo-voltaic cluster reference voltage and the underlying rotor speed reference for the wind turbine are balanced if the two systems yield power which does not match to their maximum power point [38]. It has to conform the underlying reference values in the heading of expanding way of yield power and the other way around. Until the WT and PV systems achieve the maximum power, MPPT methods considered it as an issue, then it finds the voltage VMP (maximum voltage) and current IMP (maximum current) and naturally under a given temperature and irradiance, the PV exhibit ought to get the maximum power (MP) PMP [39]. Advanced P&O algorithm has been proposed to find the optimum DC voltage and current and to track maximum power point of a wind farm with double-fed induction generator (DFIG) [40].

In this paper, MPPT is used for extracting the maximum power from the hybrid (PV–WT–FC) system and transferring that power to the load. A DC/DC converter serves the purpose of transferring maximum power from the modules to the load. A DC/DC converter acts as an interface between the load and the module. By changing the duty cycle the load impedance as seen by the source is varied and matched at the point of the peak power with the source so as to transfer the maximum power. Therefore, MPPT techniques are needed to maintain the module's operating at its MPPT. process to express reaction kinetics and electro-osmotic drag during the polymer electrolyte process. Equations (5)–(10) represent the five equations for this FC model in vector form: Figure 2. Solar Cells equivalent circuit. Energies 2021, 14, x 4 of 19 Figure 2. Solar Cells equivalent circuit. Figure 3. P–V and I–V Characteristics of solar cell for Different Irradiance for constant T=25°C. 2.2.FC Mathematical Model the FC [24] consists of Proton exchange membrane (PEM) [25–27], catalyst layer (CL), gas diffusion layer (GDL), gas channel (GC), and current collector (CC) of both anode and cathode. Figure 4 illustrates the proton exchange membrane fuel cell (PEMFC). 2.2.1. Model Equations of FC FC's fundamental model includes mass, thermal energy, momentum, organisms, and charge. This FC model is based on five equations. These equations are combined to form an electrochemical process to express reaction kinetics and electro-osmotic drag during the polymer

electrolyte process. Equations (5)–(10) represent the five equations for this FC model in vector form: Figure 3. P–V and I–V Characteristics of solar cell for Different Irradiance for constant T = 25 ◦C. 2.2. F

Continuity Equation The electrodes present in the FC are made up of carbon fiber or carbon cloth. The reactant gases are spread over the CL, and the electrodes are restrained as a porous medium everywhere. The continuity equation for the porosity with the help of electrodes (ε) has given in Equation (5).

$$\left(\frac{\partial \varepsilon \rho}{\partial t}\right) + \nabla \times (\varepsilon \rho U) = 0$$

where ∇ = differential operator of a vector, ϱ = liquid density, ε = porosity, U = floating speed vector and t=time. Momentum Conservation

Navier–Stokes equation has given in Equation (6) and designed for a Newtonian fluid

$$\left(\frac{\partial(\varepsilon \rho U)}{\partial t}\right) + \nabla \cdot \left(\varepsilon \rho U^2\right) = -\varepsilon \nabla p + \varepsilon F + \nabla \cdot (\varepsilon \tau) - \frac{\varepsilon^2 \mu U}{k}$$

where ϱ = pressure; τ = stress tensor; F = floating mass vector; μ = liquid viscidity degree; K= permeate ratio of the liquid by porous medium.

Conversion of Charge Equation PEMFC is used in CL to conduct electrochemical reactions. The charge equations are an integral part of the FC, and this equation consists of two equations: electron removal above conductive solid phase and proton transference above the membrane. The oxygen diffusion flux (ODF) on the catalyst surface is used to calculate the current density (CD) that circulates along with CL. The CL's two-dimensional Poisson's equation is as follow:

$$\nabla \cdot i = 0$$

Artificial Neural Network
Levenberg-Marquardt algorithm

The Levenberg-Marquardt algorithm is designed to work specifically with loss functions which take the form of a sum of squared errors. It works without computing the exact Hessian matrix. Instead, it works with the gradient vector and the Jacobian matrix.
Consider a loss function which takes the form of a sum of squared errors,

$$f = \sum_{i=1}^{m} e_i^2$$

Here mm is the number of training samples.
We define the Jacobian matrix of the loss function as that containing the derivatives of the errors with respect to the parameters,

$$\mathbf{J}_{i,j} = \frac{\partial e_i}{\partial \mathbf{w}_j},$$

for i=1,…,mi=1,…,m and j=1,…,nj=1,…,n.

Where mm is the number of samples in the data set, and nn is the number of parameters in the neural network. Note that the size of the Jacobian matrix is m·nm·n.
We can compute the gradient vector of the loss function as

$$\nabla f = 2\mathbf{J}^T \cdot \mathbf{e}$$

Here ee is the vector of all error terms.
Finally, we can approximate the Hessian matrix with the following expression.

$$\mathbf{H}f \approx 2\mathbf{J}^T \cdot \mathbf{J} + \lambda \mathbf{I}$$

Where $\lambda\lambda$ is a damping factor that ensures the positiveness of the Hessian and II is the identity matrix.
The next expression defines the parameters improvement process with the Levenberg-Marquardt algorithm

$$\mathbf{w}^{(i+1)} = \mathbf{w}^{(i)} - (\mathbf{J}^{(i)T} \cdot \mathbf{J}^{(i)} + \lambda^{(i)}\mathbf{I})^{-1} \cdot (2\mathbf{J}^{(i)T} \cdot \mathbf{e}^{(i)})$$

for i=0,1,…i=0,1,….

When the damping parameter $\lambda\lambda$ is zero, this is just Newton's method, using the approximate Hessian matrix. On the other hand, when $\lambda\lambda$ is large, this becomes gradient descent with a small training rate.

The parameter $\lambda\lambda$ is initialized to be large so that the first updates are small steps in the gradient descent direction. If any iteration results in a failure, then $\lambda\lambda$ is increased by some factor. Otherwise, as the loss decreases, $\lambda\lambda$ is reduced, so the Levenberg-Marquardt algorithm approaches the Newton method. This process typically accelerates the convergence to the minimum.
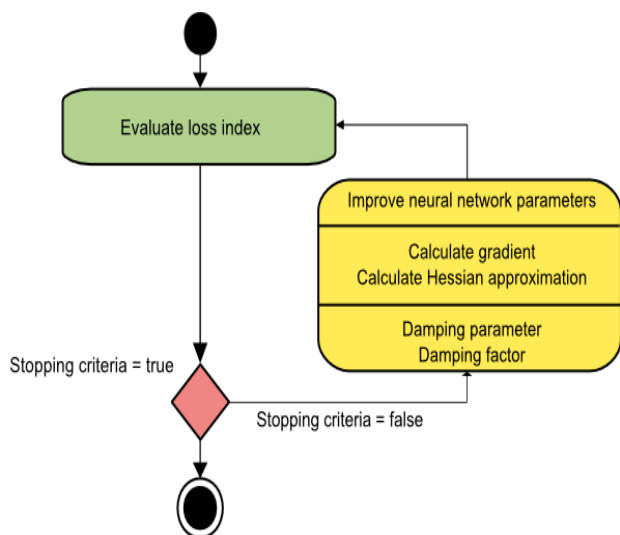

The following figure is a state diagram for the training process of a neural network with the Levenberg-Marquardt algorithm. The first step is to calculate the loss, the gradient, and the Hessian approximation. Then the damping parameter is adjusted to reduce the loss at each iteration.

As we have seen, the Levenberg-Marquardt algorithm is a method tailored for functions of the type sum-of-squared-error. That makes it to be very fast when training neural networks measured on that kind of errors.

However, this algorithm has some drawbacks. First, it cannot minimize functions such as the root mean squared error or the cross-entropy error. Also, the Jacobian matrix becomes enormous for big data sets and neural networks, requiring much memory. Therefore, the Levenberg-Marquardt algorithm is not recommended when we have big data sets or big neural networks.
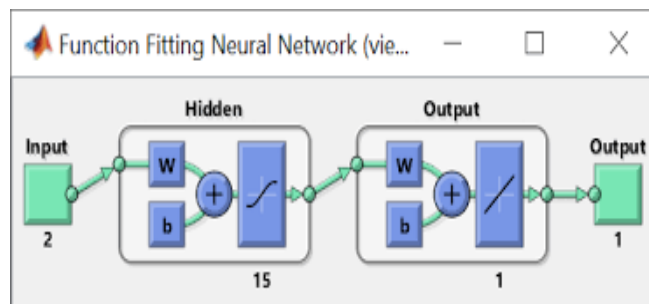
3. Results

Simulation analysis using MATLAB/Simulink is executed in favour to calculate the maximum power of the resistive load. Hybrid renewable energy system has been simulated and evaluated. simulation results of input power and input voltage before boost converter without fuzzy logic controller-based MPPT, and of input power and input voltage after boost converter with FLC and ANN-based MPPT using MATLAB/Simulink.
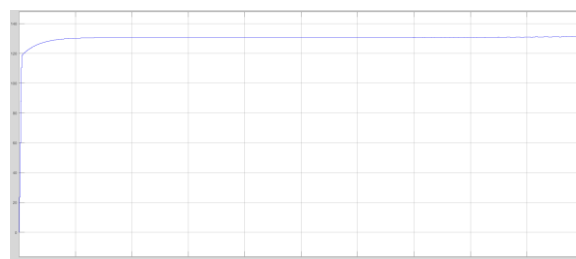
4. Conclusion and Future Scope

The paper has presented a novel MPPT in solar PV, WT, FC and proposed hybrid system that provides an accurate and fast estimation in a hybrid system. Some quality indices have been proposed in order to compare the performance of different ANN structures and they have

been computed in the case study considering numerous random generated scenarios. The results have also highlighted a good robustness of the method to parameter variations of PV system.

The result shows that MPPT technique improves the efficiency of the proposed hybrid system. The analysis of the proposed hybrid system provides higher power as compared to PV, WT and FC systems at different loads. This research is utilized for the stand-alone system as well as a grid. In future works, experimental tests of the proposed MPPT could highlight which hardware solutions are more suitable also considering the economical investment point of view. In particular, the trade-off among implementation costs and energy losses could be investigated.

References

[1]. Esram T, Chapman PL. Comparison of photovoltaic array maximum power point tracking techniques. IEEE Trans Energy Convers 2007;22(2):439–49.

[2]. De Brito MAG, Galotto L, Sampaio LP, de Azevedo e Melo G, Canesin CA. Evaluation of the main MPPT techniques for photovoltaic applications. IEEE Trans Indus Electr 2013;60(3):1156–67.

[3]. Ishaquea K, Salamb Z. A review of maximum power point tracking techniques of PV system for uniform insolation and partial shading condition. Renew Sustain Energy Rev 2013;19(March):475–88.

[4]. Jain S, Agarwal V. Comparison of the performance of maximum power point tracking schemes applied to single-stage grid-connected photovoltaic systems. IET Electr Power Appl 2007;1(5):753–62.

[5]. Femia N, Granozio D, Petrone S, Spagnuolo G, Vittelli M. Predictive & adaptive MPPT perturb and observe method. IEEE Trans Aerosp Electron Syst 2007;43(3):934–50.

[6]. Casadei D, Grandi G, Rossi C. Single-phase single-stage photovoltaic generation system based on a ripple correlation control maximum power point tracking. IEEE Trans Energy Convers 2006;21(2):562–8.

[7]. Abdelsalam AK, Massoud AM, Ahmed S, Enjeti P. High-performance adaptive perturb and observe MPPT technique for photovoltaic-based microgrids. IEEE Trans Power Electron 2011;26(4):1010–21.

[8]. Qiang M, Mingwei S, Liying L, Guerrero JM. A novel improved variable step-size incremental-resistance MPPT method for PV systems. IEEE Trans Industr Electron 2011;58(6):2427–34.

[9]. Fangrui L, Shanxu D, Fei L, Bangyin L, Yong K. A variable step size INC MPPT method for PV systems. IEEE Trans Industr Electron 2008;55(7):2622–8.

[10]. Sera D, Teodorescu R, Hantschel J, Knoll M. Optimized maximum power point tracker for fast-changing environmental conditions. IEEE Trans Industr Electron 2008;55(7):2629–37.

[11]. Weidong X, Ozog N, Dunford WG. Topology study of photovoltaic interface for maximum power point tracking. IEEE Trans Industr Electron 2007;54(3):1696–704.

[12]. Karlisa AD, Kottasb TL, Boutalisb YS. A novel maximum power point tracking method for PV systems using fuzzy cognitive networks (FCN). Electric Power Syst Res 2007;77(3–4):315–27.

[13]. Kulaksız AA, Akkaya R. A genetic algorithm optimized ANN-based MPPT algorithm for a stand-alone PV system with induction motor drive. Sol Energy 2012;86(9):2366–75.

[14]. Bahgata ABG, Helwab NH, Ahmadb GE, El Shenawyb ET. Maximum power point traking controller for PV systems using neural networks. Renew Energy 2005;30(8):1257–68.

[15]. Hiyama T, Kitabayashi K. Neural network based estimation of maximum power generation from PV module using environmental information. IEEE Trans Energy Convers 1997;12(3):241–7.

[16]. Hareesh Sita, Reddy, P Umapathi Reddy& Kiranmayi, R. (2020). Optimal location and sizing of UPFC for optimal power flow in a deregulated power system using a hybrid algorithm. International Journal of Ambient Energy,.Vol.43, No.1, pp.1413-1419, 2020..

[17]. K Krishna Reddy, D V Kiran, B Gurappa, A Nagaraju. "Modeling simulation and analysis of pv cell boost converter fed induction motor drive with closed loop speed control",Grenze ID: 02.CSPE.2015.4.28, Page(S): 127-136

[18]. Krishna Reddy, N V Kishore Kumar. "A New Z-Source Multilevel Inverter for Induction Motor Drives", IJSETR,ISSN2319-8885,Vol.04,Issue.10,April-2015, Pages:1901-1906.

[19]. K Krishna Reddy, D V Kiran. "Torque Ripple and Harmonics Reduction in BLDC Drive using Multilevel Inverter ", IJATIR, ISSN 2348–2370, Vol.07, Issue.03, April-2015, Pages: 0367-0373.